metals

Article

Energy, Environmental, Economic, and Technological Analysis of Al-GnP Nanofluid- and Cryogenic LN_2-Assisted Sustainable Machining of Ti-6Al-4V Alloy

Aqib Mashood Khan [1], Saqib Anwar [2], Muhammad Jamil [3], Mustafa M. Nasr [2], Munish Kumar Gupta [1], Mustafa Saleh [2], Shafiq Ahmad [2] and Mozammel Mia [4,*]

[1] Key Laboratory of High Efficiency and Clean Mechanical Manufacture, School of Mechanical Engineering, Jinan 250061, China; dr.aqib@nuaa.edu.cn (A.M.K.); munishgupta@sdu.edu.cn (M.K.G.)
[2] Industrial Engineering Department, College of Engineering, King Saud University, P.O. Box 800, Riyadh 11421, Saudi Arabia; sanwar@ksu.edu.sa (S.A.); mhayal@ksu.edu.sa (M.M.N.); msaleh3@ksu.edu.sa (M.S.); ashafiq@ksu.edu.sa (S.A.)
[3] College of Mechanical and Electrical Engineering, Nanjing University of Aeronautics and Astronautics, Nanjing 210016, China; engr.jamil@nuaa.edu.cn
[4] Department of Mechanical Engineering, Imperial College London, London SW7 2AZ, UK
* Correspondence: m.mia19@imperial.ac.uk

Abstract: The quest for advanced cooling/lubrication approaches for energy-efficient, eco-benign, and cost-effective sustainable machining processes is garnering attention in academia and industry. Electrical and embodied energy consumption plays an important role in reducing CO_2 emissions. In the present study, new empirical models are proposed to assess sustainable indicators. The embodied energy, environmental burden, and cost of coolant/lubricant have been added in the proposed models. Initially, optimal levels of minimum quantity lubrication (MQL) oil flow rate, liquid LN_2 flow rate, air pressure, and nanoparticle concentration were found. Based on optimal technological parameters, experiments were performed under the same cutting conditions (machining parameters) for MQL and cryogenic LN_2-assisted external turning of Ti6-Al-4V titanium alloy. The electric power and energy consumption, production time/cost, and CO_2 emissions were assessed for a unit cutting-tool life. Later, specific responses were measured and compared between both cooling and lubrication approaches. Results showed that hybrid Al-GnP nanofluid consumed 80.6% less specific cumulative energy and emitted 88.7% less total CO_2 emissions. However, cryogenic LN_2 extended tool life by nearly 70% and incurred 4.12% less specific costs with 11.1% better surface quality. In summary, after Energy–Economy–Ecology–Engineering technology (4E)-based analysis, cryogenic LN_2 is sustainable economically but not environmentally and there is a need to improve the sustainable production of LN_2 at an industrial scale to achieve environmental sustainability. The present study provides useful information to establish clean machining processes.

Keywords: sustainable manufacturing; energy consumption; energy conservation; CO_2 emission; clean environment; production cost

check for updates

Citation: Khan, A.M.; Anwar, S.; Jamil, M.; Nasr, M.M.; Gupta, M.K.; Saleh, M.; Ahmad, S.; Mia, M. Energy, Environmental, Economic, and Technological Analysis of Al-GnP Nanofluid- and Cryogenic LN_2-Assisted Sustainable Machining of Ti-6Al-4V Alloy. *Metals* **2021**, *11*, 88. https://doi.org/10.3390/met11010088

Received: 1 December 2020
Accepted: 27 December 2020
Published: 4 January 2021

1. Introduction

With the increasing population and higher demand for industrial products, energy consumption is increasing. Due to the depletion of natural resources, oil prices are increasing over time. However, the negative oil prices in the USA are an exceptional case due to COVID-19. The manufacturing sector plays an essential role in fulfilling the world demand for discrete products. Although energy prices in China did not increase significantly and the energy cost fluctuates at around CNY 0.723/kWh for the industrial sector, the carbon footprints of Chinese electric grids are very high as compared to electric grids in Europe [1]. In the world, a 56% growth in electricity demand is expected between 2010 and 2040. Consequently, CO_2 emissions will increase by 46% in the next 30 years [2]. Most of the global electricity is generated by using coal and other non-renewable resources. In the case of China, more than 70% of electricity is produced by coal, and the burning of coal has the highest carbon footprint. Besides, approximately 57% of total energy demand is accounted for by the manufacturing sector [3].

Global warming is the main concern of many climate scientists, and these concerns are pushing countries for reductions in CO_2 emissions. If these concerns are to be heeded, a significant amount of carbon emission needs to be reduced. The reduction in CO_2 in China is inevitable as it shares more than a quarter of the planet's annual greenhouse gas emissions. It is indispensable to reduce CO_2 emissions in the manufacturing sector by acting upon the Paris Agreement's guidelines. Carbon emission is the translation of electricity consumption, and the best way to reduce CO_2 emission is the reduction in energy demand. Another possible solution was to impose a "Carbon price" on carbon-based energy and it was accepted as the most effective approach for reducing CO_2 emissions. Carbon price/carbon tax is also known as an environmental cost, and it is a tax on carbon-based energy which can help to decrease the demand for energy-intensive processes or force the producer to switch to other sustainable approaches [4].

Recently, both academia and the metal processing industry are trying to cope with challenges occurring during the machining of difficult-to-cut materials. Efforts are being made to enhance the machining process' productivity at a lower cost without polluting the environment and compromising the machined part's surface quality. This can be achieved by introducing new concepts and using advanced technologies to enable efficient and effective manufacturing.

Holistic assessment aiming at energy and resource efficiency of newly developed cooling/lubrication approaches can provide a guideline for establishing a sustainable manufacturing process. The electrical energy consumption of a machine tool varies throughout the cycle time, and thus, the energy consumption profile of the machine tool is very complex (Figure 1). Various modeling methods for the assessment of energy consumption were developed at the cutting level. These models are based on the black box approach and only assess the cutting energy [5]. Machining processes are used to transform raw material into products by consuming the electrical and embodied energy of resources. Reduction in electrical energy consumption is not enough to minimize CO_2 emissions. However, the synergetic reduction in electrical and embodied energy can achieve environmental and economic sustainability. Both cost and embodied energy of cutting fluids are also high. It is imperative to find the optimal flow rate of cutting fluids to move towards an energy-efficient machining process.

Machining is one of the key manufacturing processes and is widely used in metal processing industries. The most sustainable machining processes are performed under a dry cutting environment. However, dry cutting has several problems with the workpiece quality and cutting-tool life. Thus, to address these issues, academic researchers and machinists have been seeking an alternative opportunity such as minimum quantity lubrication (MQL) and cryogenic-assisted machining is proposed to replace the traditional emulsion-based approaches. However, sustainability-based holistic assessment of hybrid alumina and graphene nanoplatelet (Al-GnP) nanofluid and the cryogenic LN_2 cooling approach and determination of optimal resource consumption for energy-efficient machining have not been investigated yet.

In recent years, researchers have developed new models to assess electrical and embodied energy consumption of machine tools [6]. However, research work on the sustainability assessment of cooling/lubrication approaches is missing. The present work deals with the Energy–Economy–Ecology–Engineering technology (4E)-based holistic sustainability assessment of cooling/lubrication approaches to produce earth-friendly products. The novelty of the present work lies in (1) the development of new empirical models for production time, energy consumption, CO_2 emission, and production cost; (2) determining optimal resource consumption for economical and energy-efficient machining processes;

(3) synergetic reduction in electrical and embodied energies; (4) holistic sustainability assessment and comparison of two different approaches based on 4E methodology.

2. Literature Review

The present section will deal with a brief literature review about energy consumption, CO_2 emissions, and production cost.

2.1. Energy Consumption

As the electrical power consumption for different components of a machine tool varies, it is difficult to determine the energy consumption demand for each component and each stage. The electrical power structures in the machining process change with the change in the machining stage.

Cooling and lubrication approaches have a significant effect on the electrical energy consumption of machine tools [7]. However, the investigation of electrical energy consumption is not enough to evaluate the sustainability of the machining processes. Thus, in recent years, researchers have included the embodied energy of consumed resources [8]. In their study, the machine tool energy was decomposed into three components, which is not enough to provide information about the energy consumption of each component and stage. Cumulative energy demand (CED) consists of two parts, i.e., direct electrical energy demand and indirect embodied energy demand. Indirect energy is associated with the cutting tool, workpiece, lubricant, lubricant preparation, cleaning, and disposal activities. In the life cycle assessment (LCA) methodology, CED is an essential key indicator to assess total energy [9].

2.2. Environmental Burden

Assessment of CO_2 emissions under holistic system boundaries is a fundamental step to reduce the environmental burden of mechanical machining processes. Carbon emission can be estimated by adopting different methods. GaBi Software [10]—the commercial software used for the life cycle costing, life cycle working environment, and life cycle assessment of products—needs a lot of accurate data for a satisfactory analysis. Ic et al. [11] conducted an experimental study to measure CO_2 emission and surface finish during the turning of 7075 aluminum alloys. Optimal cutting parameters were found considering minimal CO_2 emission and surface roughness. In another study, Yi et al. [12] studied the environmental impacts of consumed resources. The authors added the carbon footprints of the cutting-tool workpiece and coolant consumed during the machining process.

The machining process transforms raw material into useful mechanical products, and during the production of parts, CO_2 is emitted due to electrical energy consumption and utilization of cutting tools, coolants, and workpiece material. The electrical energy consumed during machining stages (direct) and embodied energy used by consumed resources (indirect) are responsible for CO_2 emission. As such, during the machining process, each machining stage and consumed resource contributes to CO_2 emissions depending upon the corresponding process time. The CO_2 emissions for disposal activities are considered zero as both MQL and cryogenic LN_2 require no disposal-related activity. The footprints of electrical energy consumption are very low as compared to the embodied energy of consumed resources [13]. Thus, for the holistic environmental sustainability of cooling/lubrication approaches, it is necessary to include the footprints of coolants and lubricants.

2.3. Production Cost

In the past, the production cost for machining products was calculated using the Taylor cost model [14]. The proposed model was only useful for dry cutting conditions and did not include the influence of coolant and lubricant on the production cost. Later, Kalpakjian and Serope [15] also worked on the assessment of production cost. The authors calculated the total sum of cutting tool cost, machining cost, and cost incurred due to change of cutting tool. With the advancement of manufacturing processes, there is a need to propose the microeconomics-level cost model. Thus, Branker et al. [16] proposed the first cost model at the microeconomics level. The author included all the traditional (tooling cost, material cost, overhead cost, and material cost) and non-traditional (energy and environmental cost) components of cost in the model. Jamil et al. [17] developed cost models for dry, minimum quantity lubrication (MQL), and cryogenic cooling approaches in the machining of titanium alloy. The results showed that the cryogenic cooling approach reduced production cost by 34% and 39% as compared to the dry and MQL approaches, respectively. Priarone et al. [6] employed a bottom-up approach (BUA) to develop cost models for the dry and wet turning of Ti-6Al-4V alloys. Optimal cutting parameters were found for the minimum specific cost, production time, CO_2 emission, and energy consumption. Recently, Khan et al. [13] calculated the production cost of the nanofluid-assisted machining process and provided a break-down of the production cost into sub-components. The authors observed that cost of consumed resources was a significant portion of the total cost. Various cooling and lubrication approaches possess their pros and cons. Thus, it is necessary to investigate and compare the holistic economic sustainability assessment of cooling/lubrication approaches.

2.4. Cooling and Lubrication Approaches

Higher material removal rates (*MRR*) should be practiced for lesser costs. However, a higher *MRR* leads to severe wear of cutting tools [18]. Each metal-processing industry has a requirement to achieve higher productivity without compromising cutting-tool life. For this purpose, advanced lubrication/cooling (lubricooling) approaches have been introduced. Nanofluid MQL (NFMQL)-assisted machining technology is garnering fame in industry and academia. Researchers enhanced the productivity of the machining process without compromising the life of the cutting tool [19]. Recently, nanoparticles have been used with conventional lubricants to obtain enhanced thermo-physical properties and achieve a reduction in friction and wear. Nanoparticles are also found to enhance heat transfer capabilities improving the efficiency of machine tools. It is a fact that cost and emission incurred by cutting tools are just a small fraction of the total cost and emissions per part [20].

Mostly, straight, soluble, semi-synthetic, and synthetic oils are either used separately or as in a hybrid cooling agent. Besides dry machining processes, some cooling/lubrication-assisted machining such as the flood cooling approach, near dry lubrication, high-pressure cooling, solid lubrication integrated with sprayed cooling, oil–water emulsion, nanofluid and hybrid nanofluids approaches are employed at machining workshops to machine hard and difficult-to-cut materials [21]. In another study, Khan et al. [22] developed new energy-integrated cost models for nanofluid-assisted machining. The authors holistically investigated the 3E-based (Energy, Environment, Economy) sustainability of the hybrid Al-GnP nanofluid-assisted machining process. In another study, Khanafer et al. [23] worked on the machinability and sustainability analysis of multi-walled carbon nanotubes (MWCNTs) and alumina oxide-based nanofluid-assisted machining. Though the authors claimed to have the lowest power using MWCNTs, neither the cost model nor the energy consumption models were formulated. The selection of nanoparticles and preparation of nanofluids are essential aspects before the application of nanofluids in the machining process. Likewise, during nanofluid preparation, the selection of base fluid and the size of nanoparticles are the two most important factors [24]. The quality of nanofluids is evaluated by investigating their important properties, such as their thermo-physical properties and their tribology (wear and coefficient of friction).

Apparently, cryogenic fluids such as CO_2 and LN_2 remove heat in the cutting zone and fluid evaporates as nitrogen gas, which is already 79% of the atmosphere. This makes cryogenic cooling (LN_2) the most eco-benign and clean approach for application in machining processes. However, it is essential to consider the embodied energy required to synthesize the unit liter of LN_2 and the corresponding environmental burden of LN_2. Damir et al. [25] developed a single score indicator evaluation method to investigate the environmental impact of cryogenic cooling assisted turning of Ti-6Al-4V. Lu et al. [26] are the first authors who investigated the effect of including embodied energy of LN_2 on the total energy consumption and compared it with the conventional emulsion approach. A state-of-art review paper published by Jawahir et al. [27], is considered as the Bible of the cryogenic assisted mechanical machining processes. The manuscript consisted of a holistic investigation of the application of cryogenics in the manufacturing process. The authors discussed the effect of LN_2 on process mechanism, material properties, quality of products produced, tribological interface interactions and thermal aspects, surface and sub-surface modification, performance enhancement, predictive model development, and economic aspects. However, the effect of LN_2 on machine tool power consumption and the cost of LN_2 was not discussed.

3. Empirical Models for Sustainable Indicators

In the past, researchers worked on the empirical modeling of a sustainable indicator. They employed the black box approach (BBA) to develop empirical models. This approach is relatively simple and it involves empirical models without considering the footprints of consumed resources. Consequently, in the BBA-based modelling approach, machine tools are considered as a black-box entity. Thus, this approach is not suitable for the holistic modeling of sustainable machining processes. However, the bottom-up approach (BUA) is holistic in nature and it considers both direct and indirect resource consumption.

In the present study, empirical models for energy, CO_2 emissions, and cost are developed using the BUA approach. Cycle time was obtained under the new system boundaries and power consumption was measured for various functionality states of a machine tool. Energy consumption was obtained based on data of cycle time and power consumption.

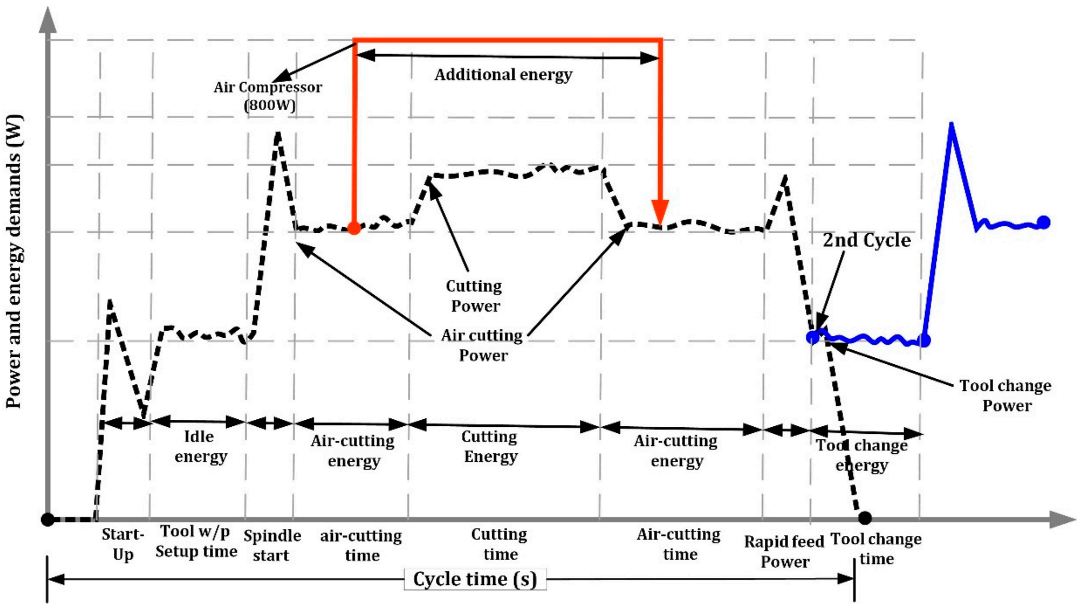

Figure 1. Power and energy consumption in various functionality states of machine tool.

Cycle time was defined as the total time required to complete a unit path from the workpiece (Figure 1). It includes idle time, air cutting time, cutting time, tool change time, and cooling/lubrication time.

$$\text{Cycle time}: \ T_{(c)} = t_{(i)} + t_{(a)} + t_{(c)} + t_{(tc)} + t_{(col/lub)} \tag{1}$$

The idle time consist of standby time, material handling time, and setup time.

$$\text{Idle time}: \ t_i = t_{sb} + t_h + t_{su} \tag{2}$$

The units, values, and definitions of all variables used in Equations (1) and (2) and the subsequent equations in this section (Equations (3)–(12)) are given in the nomenclature and Table 2.

Power consumption was considered due to various states of machine tool and it can be modelled as in Equation (3).

$$Machine\ Power\ P_{(m)} = P_{(i)}(t) + P_{(a)}(t) + P_{(c)}(t) + P_{(tc)}(t) + P_{(lub/col)}(t) \tag{3}$$

Energy consumption during the cycle time was measured and expressed as in Equation (4).

$$E_{(m)} = \int_0^{t_{(i)}} P_{(i)}(t)dt + \int_0^{t_{(a)}} P_{(a)}(t)dt + \int_0^{t_{(c)}} \left(P_{(c)} + P_{(l)}\right)(t)dt + \int_0^{t_{(tc)}} P_{(i)}(t)dt \tag{4}$$

MRR means material removal rate and *MRV* stands for material removal volume; both *MRR* and *MRV* are calculated according to Equations (5) and (6), respectively.

$$MRR = v_c \times f \times a_p \tag{5}$$

$$MRV = MRR \times t_c \tag{6}$$

Cumulative energy demand (CED) is the sum of total energy obtained from electrical energy consumption and embodied energy of resources consumed. It can be defined as in Equation (7).

$$\begin{aligned}\mathrm{CED} = \int_0^{t_{(i)}} P_{(i)}(t)dt + \int_0^{t_{(a)}} P_{(a)}(t)dt + \int_0^{t_{(c)}} \left(P_{(c)} + P_{(l)}\right)(t)dt + \int_0^{t_{(tc)}} P_{(i)}(t)dt + y_{MQL} \times Q_{MQL} \times t_c \\ + \left(y_{LN_2} \times Q_{LN_2}\right)\cdot(t_c + t_a)\end{aligned} \tag{7}$$

The specific CED (S_CED) can be defined as the unit amount of energy consumption removed per mm^3 of material removed.

$$S\_CED = \frac{\int_0^{t_{(i)}} P_{(i)}(t)dt + \int_0^{t_{(a)}} P_{(a)}(t)dt + \int_0^{t_{(c)}} \left(P_{(c)} + P_{(l)}\right)(t)dt + \int_0^{t_{(tc)}} P_{(i)}(t)dt + y_{MQL} \times Q_{MQL} \times t_c + \left(y_{LN_2} \times Q_{LN_2}\right)\cdot(t_c + t_a)}{MRV} \tag{8}$$

Carbon emission was calculated from both electrical energy consumption and embodied energy.

$$CE_P = CES \times (E_i + E_a + E_c + E_{tc} + E_l) + CF_{CT} \times \frac{t_c}{T_L} + CF_{MQL} \times Q_{MQL} \times t_c + CF_{LN_2} \times Q_{LN_2} \times (t_c + t_a) \tag{9}$$

Specific carbon emission is the amount of carbon emission released per unit amount of material removed.

$$S\_CE_P = \frac{CES \times (E_i + E_a + E_c + E_{tc} + E_l) + CF_{CT} \times \frac{t_c}{T_L} + CF_{MQL} \times Q_{MQL} \times t_c + CF_{LN_2} \times Q_{LN_2} \times (t_c + t_a)}{MRV} \tag{10}$$

Cost per part consists of energy cost, cutting cost, and resource consumption cost. It is worth mentioning that machining experiments were performed for a unit tool. Thus, for comparison purposes, the cost of the cutting tool was neglected.

$$C_P = (E_i + E_{su} + E_a + E_c + E_{tc} + E_{lub}) \times x_e + x_{CT} \times \frac{t_c}{T_L} + x_{MQL} \times Q_{MQL} \times t_c + x_{LN_2} \times Q_{LN_2} \times (t_c + t_a) + C_{env} + C_o \tag{11}$$

Similarly, for the comparison, the specific cost was calculated

$$S\_C_P = \frac{CES \times (E_i + E_a + E_c + E_{tc} + E_l) + CF_{CT} \times \frac{t_c}{T_L} + CF_{MQL} \times Q_{MQL} \times t_c + CF_{LN_2} \times Q_{LN_2} \times (t_c + t_a)}{MRV} \tag{12}$$

4. Experimentation

The present section will focus on the experimental setup, measurement of responses, and data inventory collection.

4.1. Work Material and Tooling

A rod (Ø 40 mm) of titanium alloy was used in the external turning process undercooling and lubrication conditions. A standard heat treatment procedure was performed on the workpiece before machining. The work material, after carrying out the heat treatment process [28], possessed an ultimate tensile strength, yield strength (0.2% proof stress), and elongation of 1003.48 MPa, 927.35 MPa, and 15.05 MPa respectively. The chemical composition of the material is shown in Table 1. It contains the primary alpha and inter-granular beta phase. The hardness of the workpiece was 348 $\pm$ 4 HV. The microstructure of the workpiece is shown in Figure 2. A universal testing machine (UTM) (Haida, China) was used to test the tensile strength and compressive strength of Ti-6Al-4V alloy.

Table 1. Chemical composition of (in mass percentage) of workpiece alloys [29].

Ti	V	Al	C	Fe	H	N	Y
Balance	4.02	5.85	0.01	0.20	0.0023	0.007	<0.0048

The experiments were performed on a Computer Numerical Control CNC lathe machine (BOOHI SK50P, Baoji Zhongcheng, Shanghai, China) with an input power of 5.7 kW and a maximum spindle speed of 160–1200 rpm. Uncoated carbide inserts with tool geometry (rake angle of 0° and the relief angle of 11°) were procured from Zhuzhou Cemented Carbide Cutting Tools Co., Ltd., Shanghai, China.

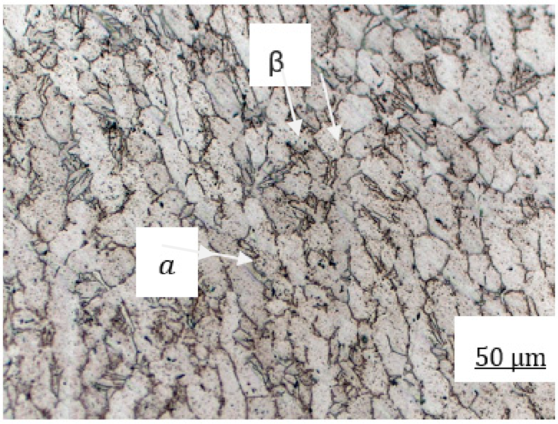

Figure 2. Optical micrographs showing the microstructure of Ti-6Al-4V alloy.

4.2. Hybrid Cooling and Lubrication Approaches

Experiments were performed under two types of cooling- and lubrication-assisted machining processes. Hybrid nanofluids (prepared by the two-step method) were procured from Sigma-Aldrich [30]. Hybrid nanofluid was impinged in the cutting zone through cutting Unilube micro lubrication systems (CH8280, Unist, NY, USA). Nanofluids were prepared with different volumetric concentrations and used immediately after preparation. It is worth mentioning that the thermal conductivity, viscosity, and coefficient of friction of the hybrid nanofluid (Al-GnP) were measured before application [22]. The Zeta potential of the Al-GnP nanoparticle was found to be 45 mV, which showed the good stability of the nanofluid.

The MQL system (applied alone) only provides efficient lubrication effects. It does not provide cooling effects at higher cutting conditions. On the other hand, cryogenic LN_2 provides good cooling and poor lubrication effects. Thus, both approaches work differently. A cylinder of liquid nitrogen (Dewar tank YD-50) was used to deliver the cryogenic medium with nozzles of various diameters (procure from Huilin company in Guangzhou, China). The extremely low temperature of −195 °C was measured at the exit of the nozzle with the help of a thermal camera. A special tube (DN20-DN2000, Huilin company, Guangzhou, China) which can bear sub-zero temperatures was used to carry LN_2 from the tank and deliver it to, a nozzle. The experimental setup with both hybrid cooling/lubrication approaches has been shown in Figure 3. It can be seen that nanofluid impinged from the MQL system.

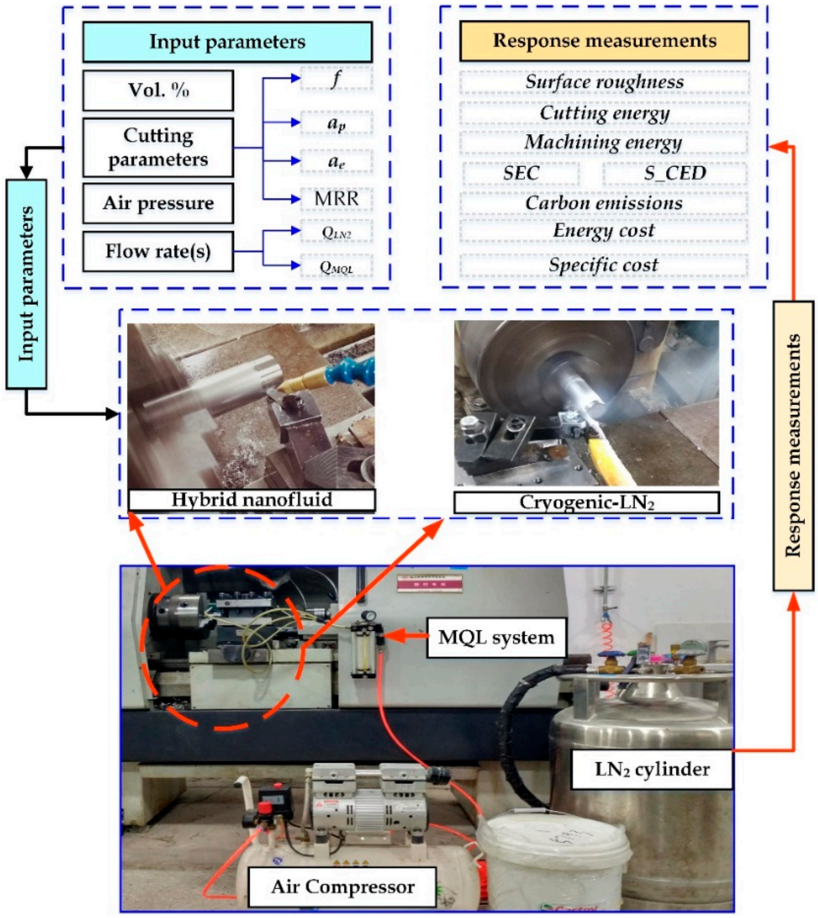

Figure 3. Experimental setup for hybrid nanofluid and cryogenic LN_2 approaches.

4.3. Experimental Procedure and Measurements

The experiments were performed under the same cutting conditions under hybrid nanofluid and cryogenic LN_2 conditions. Preliminarily experiments were performed to find the optimal flow rate, air pressure, and nanofluid concentration. A new cutting insert was used for each experiment, all experiments were performed twice, and average values were recorded to avoid errors. For the selection of optimal levels of input parameters, a cutting speed of 70 m/min, a depth of cut of 0.8 mm, and a feed rate of 0.1 mm/rev were adjusted for all experiments. However, for response measurement analysis (from Sections 5.2–5.5), cutting speed values were varied. Experiments were performed at four cutting speed values, i.e., 30, 70, 110, and 150 m/min.

Power consumption was measured for various functionality states of the machine tool. Initially, fixed standby power was measured when the machine tool was switched on but spindle and feed motors were switched off. Later, the machine tool spindle was rotated with no cutting at various speeds and power consumption was measured. Finally, air cutting power was deducted from the total machine tool power to find the cutting power. The cutting power was multiplied by the corresponding times to obtain electrical energy consumption. The power consumption was measured by using a load controls power meter. This power meter consisted of two isolated analogue outputs (0–10 V DC, 4–20 Milliamp DC). The specification of the power-measuring sensor was suitable to obtain precise data, i.e., the response time (0.015–10 s) and frequency range (1000 Hz). An optical microscope named ARTCAM and with the model 130-MT-WOM (Olympus Corporation, Tokyo, Japan) was used to measure the flank wear of the cutting inserts. When the cutting insert reached its required flank wear, cutting time was calculated to determine the life of the cutting insert. An air compressor with model number DDW30/8A (Denair company, Shanghai, China) with rated power of 800 W and a capacity of storing 30 L air was used to deliver MQL mist in the cutting region. The carbon emission signature (CES) of the Nanjing power grid station was found to be 258.2 kg CO_2/MJ. The procedure for the calculation of CO_2 emission has been adopted from ref [1].

4.4. Data Inventory

Cycle time, power, and energy consumption data were calculated, and well-known companies such as ANHO and Walter Tools from Wuxi, China were visited for validating embodied energy data related to the cutting tools. The constant values are mentioned in Table 2.

Table 2. Coefficients and fixed parameters for time, power, and energy, CO_2 emission, and cost models.

Parameter (s)	Units	Value	Reference/Remarks
$P_{(i)}$	W	350	Idle power (measured)
$P_{(col)}$	W	800	MQL system power (measured)
$t_{(i)}$	s	30	Idle time
$t_{(a)}$	s	20	Air cutting time
$t_{(tc)}$	s	60	Tool change time per part
$t_{(col/lub)}$	s	$t_c + t_a$	Lubrication time
$Q_{(LN_2)}$	L/min	0.4	LN_2 flow rate
$Q_{(MQL)}$	mL/s	300	Consumption rate of MQL oil
$y_{(LN_2)}$	MJ/L	2.6	Embodied energy LN_2 [31].
$y_{(MQL)}$	kJ/L	1.37	Embodied energy (MQL oil) [32]
CES	kg-CO_2/GJ	258.2	CES of Nanjing electric grid [33]
$CF_{(MQL)}$	kg-CO_2/L	0.11	Carbon footprints of MQL oil [34]
$CF_{(LN_2)}$	kg-CO_2/L	1.30	Carbon footprints of LN_2 [35]
$x_{(e)}$	CNY/kWh	0.723	Cost of electricity [12]
$x_{(MQL)}$	CNY/L	100	Cost of the cutting fluid
$x_{(LN_2)}$	CNY/L	1	Cost of the LN_2

5. Results and Discussion

This section deals with the selection of optimal levels of input parameters, the surface quality of the workpiece, energy consumption, CO_2 emission, and cost per part produced.

5.1. Selection of Optimal Levels of Input Parameters

The establishment of an economical cryogenic system is inevitable for the production of sustainable products. In the past, Mia et al. [35] used a very high flow rate of 20 L/min while impinging LN_2 in the cutting zone. Similarly, Sartori et al. [36] also used a cryogenic medium at 4 L/min for finishing machining the Ti6-Al-4V titanium alloy. In this study, the effect of LN_2 flow rate on cutting and machining energy was investigated and compared with dry cutting (Figure 4). It can be seen that the highest amount of power (885 W) was consumed under the dry cutting condition. Compared with dry cutting, 9.60% less cutting power and machining energy were consumed at a flow rate of 0.4 L/min. Increasing the flow rate of LN_2 from 0.4 L/min to 5 L/min results in an increase in cutting power. This phenomenon can be explained by the fact that as the LN_2 flow increases, it increases the work hardness of workpiece material. It is a well-known fact that higher cutting forces are generated while machining harder materials [37].

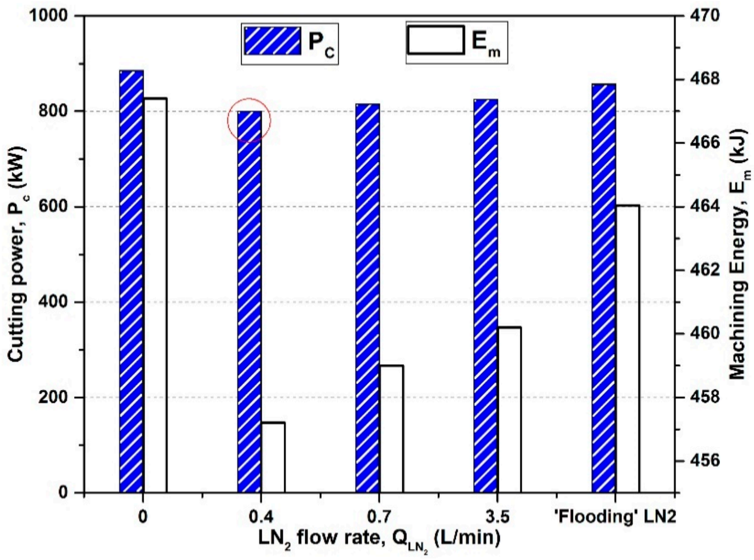

Figure 4. Influence of LN_2 flow rate on cutting power and machining energy ($v_c = 70$ m/min, $a_p = 0.8$ mm; $f = 0.1$ mm/rev).

Similar to the LN_2 flow rate, the optimal flow rate for MQL was also found. Figure 5 demonstrates the effect of MQL flow rate on cutting power and machining energy. As the MQL flow rate increases from 50 to 200 mL/h, both cutting power and machining energy decrease. However, a further increase in MQL flow rate did not affect the power. Thus, the flow rate of 200 mL/h was selected as an economical and optimal flow rate. At this flow rate, 10.6% and 2.8% less cutting power and machining energy were consumed, respectively, when compared with dry cutting (flow rate = 0 mL/h). The flow rate of 200 mL/h is optimal where the MQL system provides an effective lubrication system. Thus, a further increase in flow rate does not improve the lubrication; rather, it only adds economic burdens [38].

Besides, the structure of Blaser cutting oil consists of octadecanoic (C17H35COOH), oleic (C17H33COOH), and linoleic fatty acids (C17H31COOH). This structure helps the oil to react with workpiece metal and to develop a strong boundary lubrication layer because of its excellent adsorption capacity.

Finding the optimal mist pressure is essential for better performance of the cutting process. Keeping all cutting parameters constant and an MQL flow rate of 200 mL/h, as can be observed from Figure 6, the increase in air pressure of the MQL system also resulted in a reduction in SCE. The obtained findings are in good agreement with published research [39]. The high pressure also provides better effects in terms of enhancing the convective heat transfer which helps in chip curling. Machining energy decreases as the MQL flow rate increases. However, an MQL flow rate of more than 200 mL/h has no significant effect on the machining energy. Thus, it was found that 200 mL/h is the optimal value of flow rate for minimal energy consumption.

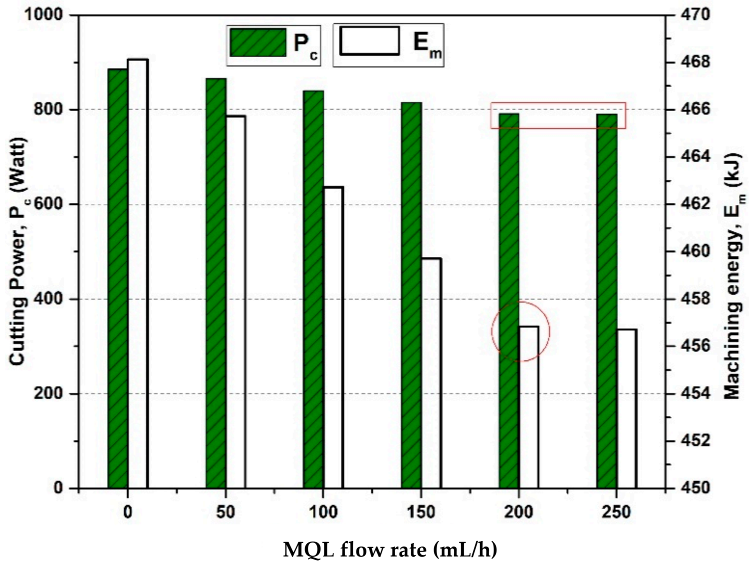

Figure 5. Effect of minimum quantity lubrication (MQL) flow rate on power and energy consumption ($v_c = 70$ m/min, $a_p = 0.8$ mm; $f = 0.1$ mm/rev; $Pp = 0.5$ MPa).

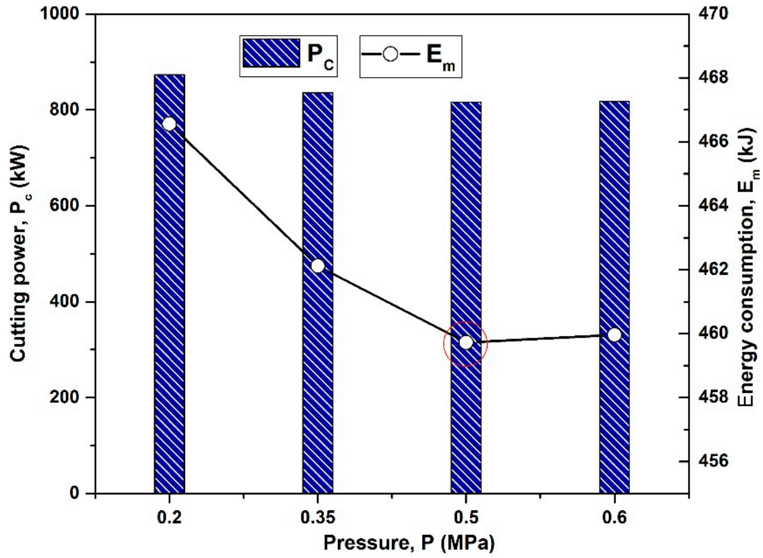

Figure 6. Effect of mist pressure on energy and power consumption ($v_c = 70$ m/min, $a_p = 0.8$ mm; $f = 0.1$ mm/rev; $n_p = 1.2$).

Figure 7 shows the schematic view of small drops and large drops due to variation in air pressure. In addition, Balan et al. [40] conducted fundamental research on the effect of air pressure in the MQL system on energy consumption in the grinding process. The authors noted that the increase in cutting pressure reduces the size of the droplets from 24.0 to 2.77 µm. In another study, it was stated that the Reynolds number significantly increases with the increase in air pressure of the MQL system, and this phenomenon further enhances the flux density at the cutting zone [41]. However, in our study, it was noted that when increasing further air pressure from 0.5 to 0.6 MPa, there was negligible change in cutting power. With the increase in pressure, energy consumption (E_m) initially increases; however, it starts decreasing at the highest level of pressure.

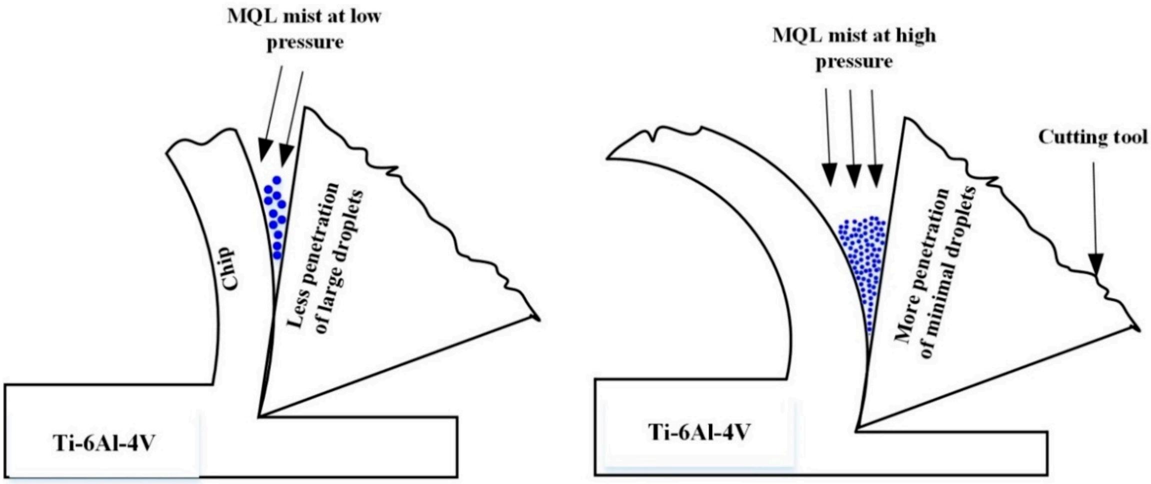

Figure 7. Effect of air pressure on airdrops at the machining zone.

The quality of nanofluid is highly influenced by the concentration of nanofluid [22]. The effect of nanofluids with various fractions of nanoparticles on cutting power and machining energy is shown in Figure 8. It can be noted that an increase in nanoparticle concentration decreases the cutting power and machining energy. This is because increasing the nanoparticle volume percentage could lead to better frictional and heat transfer behavior. In terms of frictional behavior, increasing the nanoparticle volume percentage means there are more nanoparticles in the tool–workpiece interface zone. These nanoparticles act as rollers and accordingly decrease the induced friction. Furthermore, using a higher nanoparticle volume percentage could increase the overall heat transfer coefficient and accordingly decrease the machining and cutting power, as presented in the open literature [42,43].

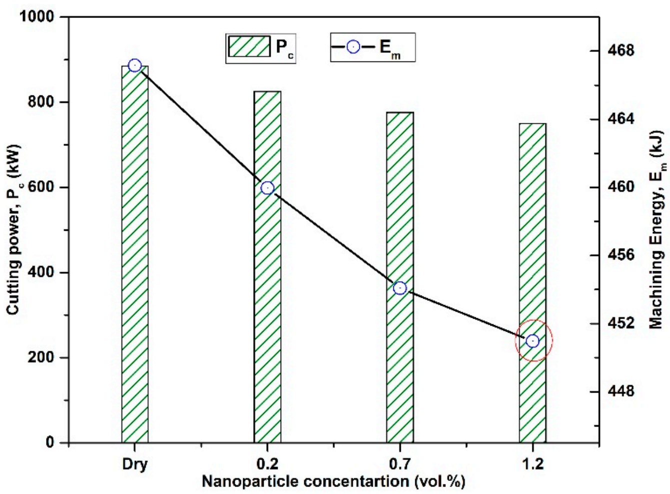

Figure 8. Effect of nanoparticles' concentration on sustainable indicators ($a_p = 0.8$ mm; $f = 0.1$ mm/rev; $P = 0.5$ MPa).

The lowest cutting power was consumed at vol.% of 1.2. At this concentration, when compared with dry cutting, cutting power and machining energy were reduced by 15.2% and 3.4%, respectively.

5.2. Mechanism of Nanofluid and Cryogenic Cooling

Numerous researchers have mentioned the potential of hybrid nanofluids regarding the improvement of machining characteristics in the cutting of difficult-to-cut materials as high cutting conditions require superior thermal conductivity, lubrication, and sustainability. Biodegradable ester oil-based nano-additives extended the heat transfer, limited the friction tool edge wear. The following mechanism played a key role in heat dissipation and the resulting high-performance machining:

- Hybrid nanofluids (variable-sized nano-additives) enhanced the performance of nanofluids behaving as spacers between the tool–workpiece contact interface.
- Hybrid nanofluids atomized through the MQL mist containing nano-additives and air mixture formed a thin tribo-film on the tool and workpiece surface to enhance the tribological characteristics.
- Hybrid nanofluids have the capability to penetrate well inside narrow surfaces, preventing rubbing of two surfaces [44].

Some complexities are also associated with the preparation of hybrid nanofluids:

- Fine dissolution of nano-additives is a challenging task.
- Nanoparticles enter our skin, cause allergies, and have a negative impact on plant growth and seeds.
- Nanoparticles are difficult to detect if opened in the air. Therefore, a hazard appraisal should also be reported to underscore the danger associated with the particles.

The cryogenic approach has phase change properties to dissipate heat from the cutting zone due to a huge difference in temperature between the cryogenic material and the surroundings. Spray cooling of cryogenic materials has the key advantage of changing phase and evaporating quickly without leaving a residue. The following characteristics or mechanisms highlight their importance in machining:

- Cryogenic materials having extremely low temperature touch the workpiece and evaporate without leaving a residue.
- The self-generated high pressure does not require external pressure.
- Quick evaporation also keeps the workpiece cold and does not affect the surrounding, creating space for the new coolant.
- Furthermore, cryogenic coolants are sustainable in machining and also improve machining under harsh cutting conditions [45].
- The Leidenfrost effect of cryogenic nitrogen also helps to improve the process efficiency.

5.3. Surface Quality

It is very necessary to keep the excellent quality of the workpiece machined surface. Average surface roughness (*Ra*) is an important metric of surface integrity evaluation. Center-line average (CLA) or the arithmetic average height parameter is mostly used to quantify the surface roughness of a workpiece and is denoted as R_a. For a specific length of sample, the average irregularities/deviations from the mean line are named as an average surface roughness (*Ra*).

Figure 9 demonstrates the effect of increasing *MRR* on the surface quality of the workpiece. The feed rate and depth of cut and technological parameters for MQL and cryogenic systems were kept constant and only cutting speed was increased from 30 to 150 m/min. It can be observed in both cutting environments that surface quality improved as the MMR increased. However, cryogenic LN_2 machining produced better surface quality as compared to hybrid nanofluid machining. At the highest cutting parameters, a 6.61% better surface roughness was achieved in the cryogenic LN_2 approach when compared with the hybrid nanofluid approach. The results are in good agreement with previous literature [46].

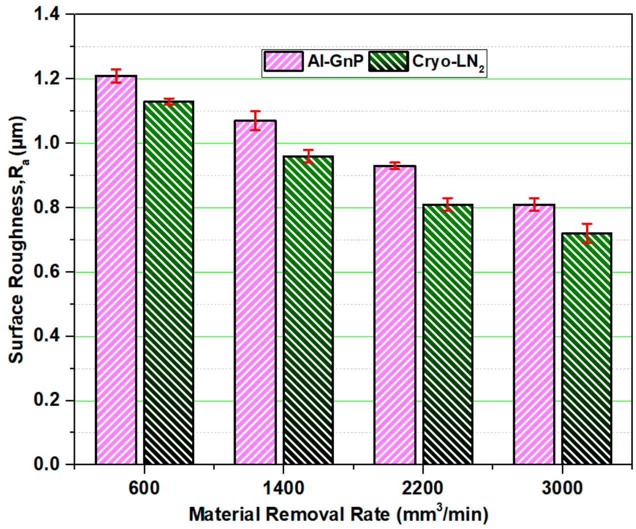

Figure 9. Comparison of the surface quality of workpieces under hybrid nanofluid- and cryogenic LN_2-assisted machining processes ($a_p = 0.8$ mm; $f = 0.1$ mm/rev; $P = 0.5$ MPa; $n_p = 1.2$).

5.4. Power and Energy Consumption

In the preliminary experiments, the optimal flow rates of LN_2 and MQL mist were found to be 0.3 L/min and 200 mL/h, respectively. Keeping technological parameters at optimal values, experiments were performed under the same cutting conditions to investigate and compare the power and energy consumed by a machine tool in a cycle time [47].

Saving electrical energy consumption means saving energy cost. From Figure 10, it can be seen that the machine tool consumes more cutting and total power under aggressive cutting conditions (*MRR* = 3000 mm^3). At the lowest cutting conditions, cryogenic-assisted machining consumed 10.7% more cutting power. However, as the cutting condition increased, cryogenic LN_2-assisted cutting consumed less power. This can be explained since as the cutting speed was increased, cycle time decreased drastically. The decrease in cycle time keeps the workpiece interacting less with LN_2 spray and it caused less workpiece hardening [48].

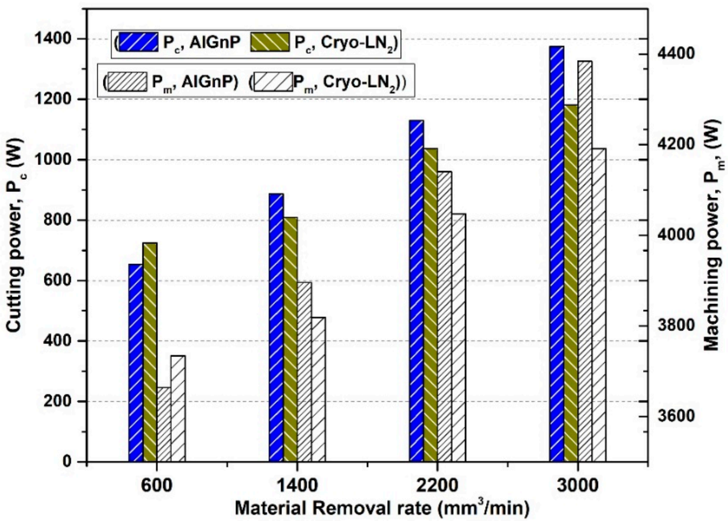

Figure 10. Effect of increasing material removal rate (*MRR*) on cutting power and machining energy in Al-GnP-assisted machining and cryogenic LN_2-assisted machining ($a_p = 0.8$ mm; $f = 0.1$ mm/rev; $P = 0.5$ MPa; $n_p = 1.2$).

Specific energy consumption (SEC) reciprocates the trends of machining power consumption. Cumulative energy demand (CED) is the total sum of electrical energy and embodied energy of used resources. From Figure 11, it is observed that as the *MRR* increases, SEC drastically decreases. This can be due to a one-third decrease in cutting time. Compared with the lowest *MRR*, the highest *MRR* had a nearly 80% lower SEC. The lower SEC for cryogenic LN_2 is due to the lower power consumption.

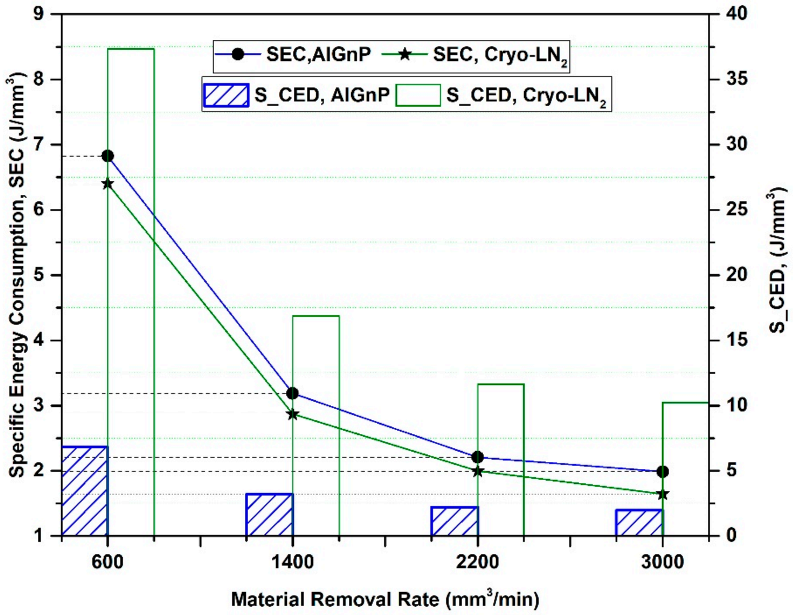

Figure 11. Influence of *MRR* on specific energy consumption (SEC) and specific cumulative energy demand (S_CED) under both environments ($a_p = 0.8$ mm; $f = 0.1$ mm/rev; $P = 0.5$ MPa; $n_p = 1.2$).

Similar to SEC, S_CED also decreased with the increase in *MRR*. However, at all cutting conditions, the hybrid Al-GnP-assisted process consumed much less S_CED as compared to the cryogenic LN_2-assisted process. The processing of liquid nitrogen is a highly energy-intensive process. Nearly 2.6 million Joules of energy is required for the synthesis of one liter of LN_2. Due to the unsustainable production of LN_2, cryogenic LN_2 consumed 447.02% more S_CED at the lowest *MRR*. However, at the highest *MRR* (vc = 150 mm/min), cryogenic LN_2 produces a longer tool life. Thus, at the highest *MRR*, cryogenic LN_2 consumed 72.5% more S_CED when compared with the lowest *MRR*.

5.5. Environmental Impacts

A "clean process" means a process that produces low carbon emissions. Both Al-GnP- and cryogenic-LN_2-assisted machining processes are considered as clean and sustainable in general. In this study, efforts were made to investigate the environmental impacts of cooling/lubrication approaches. S_CE_e is the specific carbon emission due to electrical energy consumption, and S_CE_P is the amount of total CO_2 emitted per part produced. The study was conducted in the Advanced Cutting Technologies laboratory of Nanjing city, China. For that reason, the CES value of 258.35 kg CO_2/MJ for the Nanjing power grid station was used [34].

Figure 12 illustrates the effect of increasing *MRR* on CO_2 emission. The increase in the cutting speed decreases the S_CE_e, which agrees with Ic et al. [11]. The carbon footprint of the electrical energy consumption of the Al-GnP approach is relatively higher than that of the cryogenic approach. However, the cryogenic LN_2 approach produces higher CO_2 emissions at all cutting conditions. At the highest *MRR*, cryogenic LN_2 produced 415.6% more CO_2 as compared to the Al-GnP approach.

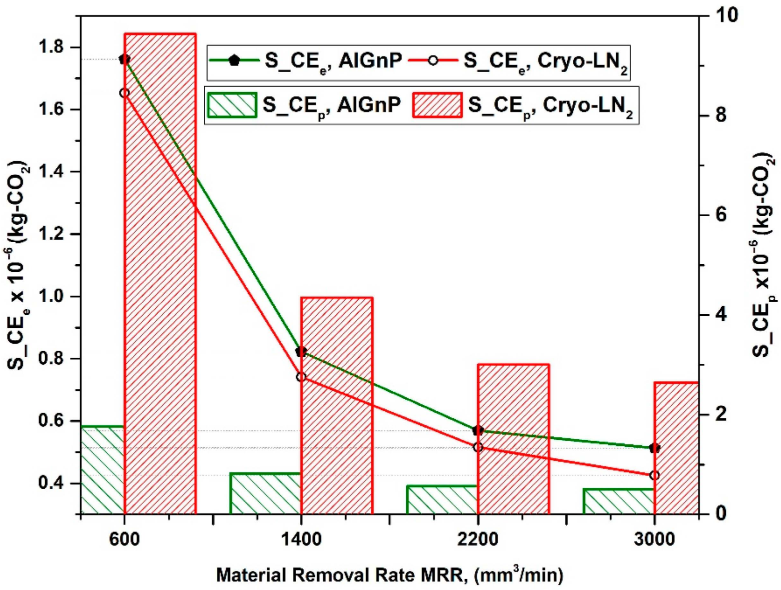

Figure 12. Influence of *MRR* on carbon footprint of electrical energy consumption and CO_2 emissions per part ($a_p = 0.8$ mm; $f = 0.1$ mm/rev; $p = 0.5$ MPa; $n_p = 1.2$).

The very high CO_2 emissions per part in the cryogenic approach are due to the unsustainable liquid nitrogen production and its larger environmental footprints. It is important to mention that for the synthesis of each 1 kg LN_2, nearly 0.67 kg CO_2 is emitted in space. Thus, it can be said that it is imperative to improve sustainable production of LN_2 for producing earth-friendly products.

5.6. Production Cost

Production cost is the sum of electricity cost, cost of consumed resources, and environmental cost. Specific energy cost mimics the trends of energy consumption. However, specific production cost highly depends upon the cost of consumed resources. The holistic cost model was developed in a previous study [49]. However, this study mainly deals with the comparison of the economic aspects of the hybrid nanofluid (MQL lubrication) and the cryogenic LN_2 cooling approaches. Thus, the cost of the workpiece, cutting tool, and the overhead cost were considered constant.

Material removal rate (*MRR*) strongly influences production costs. This is because at higher *MRR*s, cutting tools wear quickly due to the increase in friction and heat generation in the cutting zone [50]. The production cost also highly depends on the type and composition of cutting fluid. In addition, workpiece hardness, cutting parameters, and cutting tool type also affect the production cost.

It is pertinent to mention that in the present study, two sets of experiments were performed under the same cutting conditions to compare and evaluate the economic aspects. Unlike [13], a relatively small system boundary is considered.

From Figure 13, it can be seen that as more material is removed, the costs decreased. The minimum energy cost is achieved at the highest values of *MRR*. At all cutting conditions, the Al-GnP approach incurred a lower specific energy cost as compared to the cryogenic approach. For specific production cost, similar (decreasing with increase in *MRR*) trends were observed. However, the Al-GnP approach incurred 40.5%, 36.8%, and 37.11% less specific production cost at lower, medium, and high *MRR*s, respectively. At a very high *MRR* (3000 mm^3/min), cryogenic LN_2-assisted machining produced 4.14% lower-price products. Even though cryogenic LN_2-assisted machining yielded longer tool life, its higher energy consumption and the production cost of LN_2 make it expensive. Under the considered system boundary, the cost of liquid nitrogen comprises nearly one-third of the total production cost.

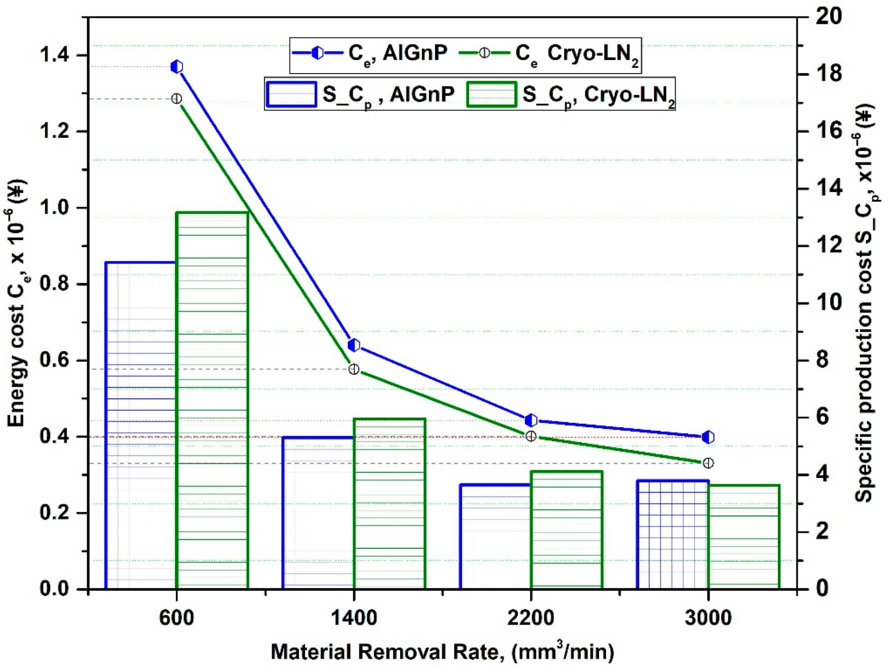

Figure 13. Comparison of energy cost and specific production cost under two various cooling/lubrication approaches ($a_p = 0.2$ mm; $f = 0.1$ mm/rev; $p = 0.5$ MPa; $n_p = 1.2$).

On the other hand, the concentration of nanoparticles has the smallest effect on the cost. As discussed in our previous study [45], nanoparticles have a significant effect on tool wear and tool life. However, in the present study, since the cutting time was shorter and a minimal amount of nanoparticles was used, a lesser effect of nanoparticles' concentration has been noted on the total cost.

6. Overall Comparison of Cooling/Lubrication Approaches

A holistic comparison of hybrid Al-GnP and cryogenic LN_2 approaches was plotted at higher cutting conditions. It is worth mentioning that all experiments were performed at the same higher cutting conditions ($a_p = 0.8$ mm; $f = 0.1$ mm/rev; $P = 0.5$ MPa; $v_c = 150$ m/min). Thus, the material removal rate was kept constant. Experiments were performed until the tool wear reached the end of its life. The Taylor tool life formula does not provide accurate results; therefore, real-time experiments were used to avoid errors. When the tool wear was very near to 300 µm, interpolation and extrapolation methods were used. The total energy consumption, total carbon emissions, and cost were calculated. However, due to different tool lives, both approaches yielded a different amount of removed material. To obtain specific energy, specific CO_2 emissions, and specific cost, the ratio of measured total response and *MRV* were obtained. The specific responses are necessary to estimate the processes' efficiencies.

From Figure 14, it can be seen that only two responses, tool life (TL) and material removed (*MRV*), are required at higher values for better outcomes, and all other sustainable metrics are required at minimal values. It is noted that the process performance of the cryogenic LN_2 approach is much better in terms of machinability. More specifically, the cryogenic LN_2 approach produced 11.1% better surface quality and 21.5% lower temperature. Additional experiments were performed to measure the temperature in the cutting zone. In addition, cryogenic LN_2 enhanced the tool life by 70.8% and removed 70.5% more material with a single cutting tool. However, cryogenic coolant production is not environmentally sustainable. That is why the Al-GnP-assisted machining emitted 88.7% less total CO_2 and 80.6% less specific CO_2.

It is important to mention that cryo-LN_2 provides excellent cooling at a workpiece cutting tool interface. The Leidenfrost effect of LN_2 spray helps to reduce the cutting temperature. The highest S_CED and S_CE are the big question mark on the application of LN_2 in the machining process. From the results, it can be said the hybrid Al-GnP-assisted machining is eco-benign and environmentally friendly. The results also emphasize that sustainable production of LN_2 is imperative for the sustainable application of LN_2 in the machining process. Even though LN_2 is much more expensive than conventional MQL oil, the cryo-LN_2 approach yielded a 4.12% lower specific cost. This is because of the longer tool life and higher productivity.

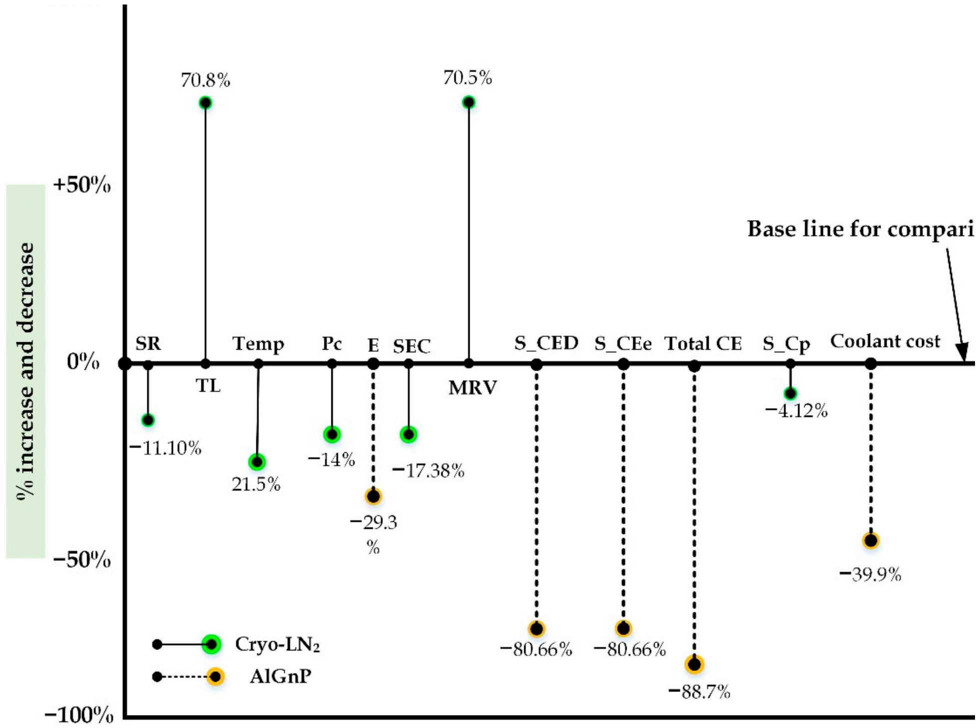

Figure 14. A holistic comparison between hybrid Al-GnP and cryogenic LN_2 at higher cutting conditions ($a_p = 0.8$ mm; $f = 0.1$ mm/rev; $P = 0.5$ MPa; $v_c = 150$ m/min).

The holistic comparison is further explained in the radar graph in Figure 15. A total of 15 metrics are compared in the radar graph. Data for operator health and safety and part cleaning were obtained from the local Chinese manufacturing industry.

Figure 15 also shows that the cryo-LN_2 approach is sustainable economically but not environmentally. It is pertinent to mention that in the 4E methodology, the fourth E represents engineering technology. The engineering technology used in hybrid nanofluid-MQL-assisted machining is well known and commonly used by many industries. However, efforts are needed to make more economical and efficient technology for LN_2 production, storage, and transport. On the one side, nanofluids are difficult to synthesize and use. On the other side, LN_2 gas can be the byproduct of the air liquefaction process. However, its production is energy-intensive, which is not environmentally friendly when it is produced for industrial application where bulk quantities are required. Thus, it is noted that both cooling (cryogenic LN_2) and lubrication (Al-GnP) approaches have some limitations in terms of engineering technologies (fourth E). If these limitations are removed from engineering aspects, both cooling and lubrication approaches are the best alternatives of the conventional emulsion-assisted machining process [51].

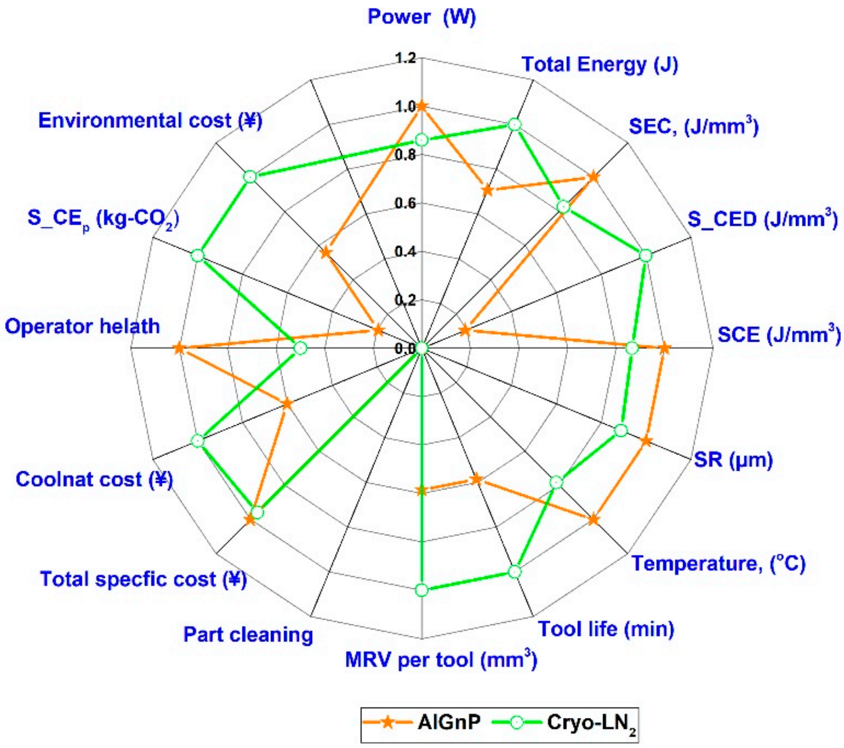

Figure 15. Radar graph to evaluate overall process performance ($a_p = 0.8$ mm; $f = 0.1$ mm/rev; $P = 0.5$ MPa; $v_c = 150$ m/min).

7. Conclusions

International Standard Organization (ISO) 14995 deals with the environmental evaluation of manufacturing processes and machine tools. In the present study, a holistic sustainability assessment of lubrication (Al-GnP nanofluid) and cooling (cryogenic LN_2) approaches was investigated. New empirical models have been proposed for energy, CO_2 emission, and production cost. Experiments were performed under the same cutting conditions, and in both cutting environments, surface quality, energy, environmental, economic, and technological perspectives of Al-GnP nanofluid- and cryogenic LN_2-assisted machining were measured and compared. Based on the obtained results, the following conclusions can be drawn.

1. The results showed that the flow rate of cryogenic LN_2 has a significant effect on energy consumption and a flow rate of more than 0.3 L/min is not sustainable economically and environmentally. Similarly, the optimal flow rate of MQL mist is also essential for economical production.
2. Owing to effective cooling effects, the cryogenic LN_2-assisted turning process produced a better surface quality of the workpiece. However, the hybrid Al-GnP produced only a few microns more than that of the cryogenic LN_2 approach.
3. At the lowest cutting parameters, the cryogenic cooling approach consumed more power. However, at very high cutting conditions, the Al-GnP approach consumed more power. The specific cumulative energy demand was very high in the cryogenic cooling approach and makes this cooling approach not sustainable. The higher CO_2 emissions in the cryogenic cooling approach are due to the high embodied energy of liquid nitrogen.
4. Procurement of liquid nitrogen is expensive as compared to MQL oil. Thus, the application of the cryogenic coolant is only economical at the highest cutting condition. The Al-GnP approach incurred less specific production cost at low, medium, and high *MRR*s. However, at very high *MRR* (3000 mm^3/min), cryogenic LN_2-assisted machining produced 4.14% lower price products.

5. In conclusion, the cryogenic LN_2 cooling approach enhanced the tool life and reduced cutting power, SEC, the tool chip temperature, and specific production cost. At the same time, higher CO_2 emissions are associated with the energy-intensive non-sustainable production of LN_2.
6. At cutting speed $v_c = 150$ m/min, the cryogenic approach outperformed in all sustainable metrics except specific cumulative energy demand and specific carbon emission. This was due to the extremely high embodied energy and carbon footprints associated with the production of liquid nitrogen.

8. Future Recommendation

In future research, a heuristic algorithm will be proposed which does not integrate the machining responses with sustainable indicators to obtain optimal cutting parameters. In addition, pressure head losses and transportation of liquid nitrogen will also be considered in a future study. Life cycle assessment (LCA) of these lubricooling approaches can be applied considering milling, drilling, and deep-hole drilling techniques. The recyclability of Al-GnP nanoparticles and personnel health and safety aspects will be addressed in the future.

Author Contributions: Conceptualization, A.M.K. and S.A. (Saqib Anwar); data curation, M.J.; formal analysis, A.M.K.; funding acquisition, S.A. (Saqib Anwar), S.A. (Shafiq Ahmad) and M.M.; investigation, A.M.K. and M.K.G.; methodology, M.J.; project administration, S.A. (Saqib Anwar) and S.A. (Shafiq Ahmad); resources, A.M.K.; software, A.M.K. and M.M.N.; supervision, M.M.; validation, S.A. (Saqib Anwar); visualization, M.K.G. and M.S.; writing—original draft, A.M.K. and M.S.; writing—review and editing, S.A. (Saqib Anwar), M.M.N. and S.A. (Shafiq Ahmad). All authors have read and agreed to the published version of the manuscript.

Funding: The authors extend their appreciation to the Deanship of Scientific Research at King Saud University for funding this work through research group no. RG-1438-088.

Institutional Review Board Statement: Not applicable.

Informed Consent Statement: Not applicable.

Data Availability Statement: Not applicable.

Acknowledgments: The authors would like to acknowledge the efforts made by I.S Jawahir of the University of Kentucky and Editor-in-Chief of "Machining Science of technology" for his valuable suggestions to improve the manuscript. The authors extend their appreciation to the Deanship of Scientific Research at King Saud University for funding this work through research group no. RG-1438-088.

Conflicts of Interest: The authors declare no conflict of interest.

Nomenclature

Symbols			
$T_{(c)}$	Cycle time (s)	$t_{(sb)}$	Standby time (s)
$t_{(i)}$	Idle time (s)	$t_{(c)}$	Cutting time (s)
$t_{(a)}$	Air-cutting time (s)	$t_{(col/lub)}$	Lubrication/coolant time (s)
$l_{(c)}$	Cutting length (mm)	$l_{(a)}$	Air-cutting length (mm)
$t_{(tc)}$	Tool change time (s)	$T_{(L)}$	Tool life (s)
MRV	Material Removal Volume (mm^3)	$P_{(sb)}$	Standby power (W)
$P_{(t)}$	Total power (W)	$P_{(su)}$	Setup power (W)
$P_{(i)}$	Idle power(W)	$P_{(c)}$	Power during cutting (W)
$P_{(a)}$	Air-cutting power (W)	$P_{(col/lub)}$	Compressor/coolant pump power (W)

Symbols			
$P_{(tc)}$	Tool change power(W)	$E_{(m)}$	Machining energy (J)
$y_{(MQL)}$	Embodied energy of MQL oil (kJ)	$y_{(LN_2)}$	Embodied energy of LN_2 (MJ)
$x_{(MQL)}$	cost of MQL oil (kJ)	$x_{(LN_2)}$	cost of LN_2 (MJ)
$CF_{(MQL)}$	Carbon footprints of MQL oil (kg-CO_2)	$CF_{(LN_2)}$	Carbon footprints of LN_2 (kg-CO_2)
CED	Cumulative energy demand (J)	S_CED	Specific cumulative energy demand (J/mm^3)
CE_P	Carbon emission per part (kg-CO_2)	S_CE_P	Specific carbon emission per part (kg CO_2/mm^3)
C_P	Total cost per part (CNY)	S_C_P	Total cost per part (CNY/mm^3)
C_{env}	Environmental cost (CNY)	C_o	Overhead costs (CNY)
Q_{MQL}	Flow rate of MQL oil (mL/hr	Q_{LN_2}	Flow rate of LN_2 (L/min)
E_i	Idle energy consumption (J)	E_{su}	Setup energy consumption (J)
E_a	Air-cutting energy consumption (J)	E_{tc}	Tool-change energy consumption (J)
E_{col}	Cooling energy consumption (J)	E_{lub}	Lubrication energy consumption (J)

References

1. Jeswiet, J.; Kara, S. Carbon emissions and CES™ in manufacturing. *CIRP Ann. Manuf. Technol.* **2008**, *57*, 17–20. [CrossRef]
2. IEA. *Energy Efficiency 2018: Analysis and Outlooks to 2040*; International Energy Agency IEA: Paris, France, 2018. Available online: https://www.iea.org/reports/energy-efficiency-2018 (accessed on 12 December 2020).
3. Hu, X.; Chong, H.Y.; Wang, X. Sustainability perceptions of off-site manufacturing stakeholders in Australia. *J. Clean. Prod.* **2019**, *227*, 346–354. [CrossRef]
4. He, L.; Shen, J.; Zhang, Y. Ecological vulnerability assessment for ecological conservation and environmental management. *J. Environ. Manag.* **2018**, *206*, 1115–1125. [CrossRef] [PubMed]
5. Khan, A.M.; He, N.; Zhao, W.; Jamil, M.; Xia, H.; Meng, L.; Gupta, M.K. Cryogenic-LN_2 and conventional emulsion assisted machining of hardened steel: Comparison from sustainability perspective. *Proc. Inst. Mech. Eng. Part B J. Eng. Manuf.* **2020**. [CrossRef]
6. Priarone, P.C.; Robiglio, M.; Settineri, L. On the concurrent optimization of environmental and economic targets for machining. *J. Clean. Prod.* **2018**, *190*, 630–644. [CrossRef]
7. Kishawy, H.A.; Hegab, H.; Deiab, I.; Eltaggaz, A. Sustainability assessment during machining Ti-6Al-4V with nano-additives-based minimum quantity lubrication. *J. Manuf. Mater. Process.* **2019**, *3*, 61. [CrossRef]
8. Liu, Z.Y.; Li, C.; Fang, X.Y.; Guo, Y.B. Cumulative energy demand and environmental impact in sustainable machining of inconel superalloy. *J. Clean. Prod.* **2018**, *181*, 329–336. [CrossRef]
9. Frischknecht, R.; Wyss, F.; Büsser Knöpfel, S.; Lützkendorf, T.; Balouktsi, M. Cumulative energy demand in LCA: The energy harvested approach. *Int. J. Life Cycle Assess.* **2015**, *20*, 957–969. [CrossRef]
10. Li, Z.-G.; Cheng, H.; Gu, T.-Y. Research on dynamic relationship between natural gas consumption and economic growth in China. *Struct. Chang. Econ. Dyn.* **2019**, *49*, 334–339. [CrossRef]
11. Ic, Y.T.; Saraloğlu Güler, E.; Cabbaroğlu, C.; Dilan Yüksel, E.; Maide Sağlam, H. Optimisation of cutting parameters for minimizing carbon emission and maximising cutting quality in turning process. *Int. J. Prod. Res.* **2018**, *56*, 4035–4055. [CrossRef]
12. Yi, Q.; Li, C.; Tang, Y.; Chen, X. Multi-objective parameter optimization of CNC machining for low carbon manufacturing. *J. Clean. Prod.* **2015**, *95*, 256–264. [CrossRef]
13. Khan, A.M.; Jamil, M.; Mia, M.; He, N.; Zhao, W.; Gong, L. Sustainability-based performance evaluation of hybrid nanofluid assisted machining. *J. Clean. Prod.* **2020**, *257*, 120541. [CrossRef]
14. Tipnis, V.A. Product Life Cycle Economic Models—Towards a Comprehensive Framework for Evaluation of Environmental Impact and Competitive Advantage. *CIRP Ann.* **1991**, *40*, 463–466. [CrossRef]
15. Kalpakjian, S.; Schmid, S. *Manufacturing Engineering and Technology*, 6th ed.; Addision-Wesley Publishing Company Inc.: Boston, MA, USA, 1995; ISBN 978-0133128741.
16. Branker, K.; Adams, D.; Jeswiet, J. Initial analysis of cost, energy and carbon dioxide emissions in single point incremental forming—Producing an aluminium hat. *Int. J. Sustain. Eng.* **2012**, *5*, 188–198. [CrossRef]
17. Jamil, M.; Khan, A.M.; He, N.; Li, L.; Iqbal, A.; Mia, M. Evaluation of machinability and economic performance in cryogenic-assisted hard turning of α-β titanium: A step towards sustainable manufacturing. *Mach. Sci. Technol.* **2019**, *23*, 1022–1046. [CrossRef]
18. Sharma, V.S.; Dogra, M.; Suri, N.M. Cooling techniques for improved productivity in turning. *Int. J. Mach. Tools Manuf.* **2009**, *49*, 435–453. [CrossRef]
19. Hegab, H.; Umer, U.; Deiab, I.; Kishawy, H. Performance evaluation of Ti–6Al–4V machining using nano-cutting fluids under minimum quantity lubrication. *Int. J. Adv. Manuf. Technol.* **2018**, 4229–4241. [CrossRef]
20. Guo, H.; Qian, K.; Cai, A.; Tang, J.; Liu, J. Ordered gold nanoparticle arrays on the tip of silver wrinkled structures for single molecule detection. *Sens. Actuators B Chem.* **2019**, *300*, 126846. [CrossRef]

21. Liew, P.J.; Shaaroni, A.; Sidik, N.A.C.; Yan, J. An overview of current status of cutting fluids and cooling techniques of turning hard steel. *Int. J. Heat Mass Transf.* **2017**, *114*, 380–394. [CrossRef]
22. Khan, A.M.; Gupta, M.K.; Hegab, H.; Jamil, M.; Mia, M.; He, N.; Song, Q.; Liu, Z.; Pruncu, C.I. Energy-based cost integrated modelling and sustainability assessment of Al-GnP hybrid nanofluid assisted turning of AISI52100 steel. *J. Clean. Prod.* **2020**, *257*, 120502. [CrossRef]
23. Khanafer, K.; Eltaggaz, A.; Deiab, I.; Agarwal, H.; Abdul-latif, A. Toward sustainable micro-drilling of Inconel 718 superalloy using MQL-Nanofluid. *Int. J. Adv. Manuf. Technol.* **2020**, *107*, 3459–3469. [CrossRef]
24. Kalita, P.; Malshe, A.P.; Arun Kumar, S.; Yoganath, V.G.; Gurumurthy, T. Study of specific energy and friction coefficient in minimum quantity lubrication grinding using oil-based nanolubricants. *J. Manuf. Process.* **2012**, *14*, 160–166. [CrossRef]
25. Damir, A.; Sadek, A.; Attia, H. Characterization of Machinability and Environmental Impact of Cryogenic Turning of Ti-6Al-4V. *Procedia CIRP* **2018**, *69*, 893–898. [CrossRef]
26. Lu, T.; Kudaravalli, R.; Georgiou, G. Cryogenic Machining through the Spindle and Tool for Improved Machining Process Performance and Sustainability: Pt. II, Sustainability Performance Study. *Procedia Manuf.* **2018**, *21*, 266–272. [CrossRef]
27. Jawahir, I.S.; Attia, H.; Biermann, D.; Duflou, J.; Klocke, F.; Meyer, D.; Newman, S.T.; Pusavec, F.; Putz, M.; Rech, J.; et al. Cryogenic manufacturing processes. *CIRP Ann. Manuf. Technol.* **2016**, *65*, 713–736. [CrossRef]
28. Cai, C.; Wu, X.; Liu, W.; Zhu, W.; Chen, H.; Qiu, J.C.D.; Sun, C.-N.; Liu, J.; Wei, Q.; Shi, Y. Selective laser melting of near-α titanium alloy Ti-6Al-2Zr-1Mo-1V: Parameter optimization, heat treatment and mechanical performance. *J. Mater. Sci. Technol.* **2020**, *57*, 51–64. [CrossRef]
29. Cai, C.; Gao, X.; Teng, Q.; Kiran, R.; Liu, J.; Wei, Q.; Shi, Y. Hot isostatic pressing of a near α-Ti alloy: Temperature optimization, microstructural evolution and mechanical performance evaluation. *Mater. Sci. Eng. A* **2020**, 140426. [CrossRef]
30. Guo, H.; Li, X.; Zhu, Q.; Zhang, Z.; Liu, Y.; Li, Z.; Wen, H.; Li, Y.; Tang, J.; Liu, J. Imaging nano-defects of metal waveguides using the microwave cavity interference enhancement method. *Nanotechnology* **2020**, *31*, 455203. [CrossRef]
31. Shen, S.; Wolsky, A.M. Energy and Materials Flows in the Production of Liquid and Gaseous Oxygen. Available online: https://www.osti.gov/scitech/servlets/purl/6574363 (accessed on 6 June 2019).
32. Pusavec, F.; Kramar, D.; Krajnik, P.; Kopac, J. Transitioning to sustainable production—Part II: Evaluation of sustainable machining technologies. *J. Clean. Prod.* **2010**, *18*, 1211–1221. [CrossRef]
33. Li, C.; Tang, Y.; Cui, L.; Li, P. A quantitative approach to analyze carbon emissions of CNC-based machining systems. *J. Intell. Manuf.* **2015**, *26*, 911–922. [CrossRef]
34. Narita, H.; Kawamura, H.; Chen, L.; Fujimoto, H.; Norihisa, T.; Hasebe, T. Development of Prediction System of Environmental Burden for Machine Tool Operation (2nd Report, Proposal of Evaluation Indicator for Eco-Efficiency). *Trans. Japan Soc. Mech. Eng. Ser. C* **2006**, *72*, 923–928. [CrossRef]
35. Mia, M.; Gupta, M.K.; Lozano, J.A.; Carou, D.; Pimenov, D.Y.; Królczyk, G.; Khan, A.M.; Dhar, N.R. Multi-objective optimization and life cycle assessment of eco-friendly cryogenic N2 assisted turning of Ti-6Al-4V. *J. Clean. Prod.* **2019**, *210*, 121–133. [CrossRef]
36. Sartori, S.; Ghiotti, A.; Bruschi, S. Hybrid lubricating/cooling strategies to reduce the tool wear in finishing turning of difficult-to-cut alloys. *Wear* **2017**, *376*, 107–114. [CrossRef]
37. Iqbal, A.; Biermann, D.; Abbas, H.; Al-Ghamdi, K.A.; Metzger, M. Machining β-titanium alloy under carbon dioxide snow and micro-lubrication: A study on tool deflection, energy consumption, and tool damage. *Int. J. Adv. Manuf. Technol.* **2018**. [CrossRef]
38. Hong, S.Y. Economical and Ecological Cryogenic Machining. *J. Manuf. Sci. Eng.* **2002**, *123*, 331–338. [CrossRef]
39. Shiva Sai, S.; Manojkumar, K.; Ghosh, A. Assessment of spray quality from an external mix nozzle and its impact on SQL grinding performance. *Int. J. Mach. Tools Manuf.* **2015**, *89*, 132–141. [CrossRef]
40. Balan, A.S.S.; Kullarwar, T.; Vijayaraghavan, L.; Krishnamurthy, R. Computational fluid dynamics analysis of MQL spray parameters and its influence on superalloy grinding. *Mach. Sci. Technol.* **2017**, *21*, 603–616. [CrossRef]
41. Su, G.S.; Guo, Y.K.; Song, X.L.; Tao, H. Effects of high-pressure cutting fluid with different jetting paths on tool wear in cutting compacted graphite iron. *Tribol. Int.* **2016**, *103*, 289–297. [CrossRef]
42. Eltaggaz, A.; Hegab, H.; Deiab, I.; Kishawy, H.A. Hybrid nano-fluid-minimum quantity lubrication strategy for machining austempered ductile iron (ADI). *Int. J. Interact. Des. Manuf.* **2018**, *12*, 1273–1281. [CrossRef]
43. Hegab, H.; Umer, U.; Soliman, M.; Kishawy, H.A. Effects of nano-cutting fluids on tool performance and chip morphology during machining Inconel 718. *Int. J. Adv. Manuf. Technol.* **2018**, *96*, 3449–3458. [CrossRef]
44. Yang, W.; Pudasainee, D.; Gupta, R.; Li, W.; Wang, B.; Sun, L. An overview of inorganic particulate matter emission from coal/biomass/MSW combustion: Sampling and measurement, formation, distribution, inorganic composition and influencing factors. *Fuel Process. Technol.* **2020**, 106657. [CrossRef]
45. Lv, Q.; Liu, H.; Yang, D.; Liu, H. Effects of urbanization on freight transport carbon emissions in China: Common characteristics and regional disparity. *J. Clean. Prod.* **2019**, *211*, 481–489. [CrossRef]
46. Jamil, M.; Khan, A.M.; Hegab, H.; Gong, L.; Mia, M.; Gupta, M.K.; He, N. Effects of hybrid Al_2O_3-CNT nanofluids and cryogenic cooling on machining of Ti–6Al–4V. *Int. J. Adv. Manuf. Technol.* **2019**. [CrossRef]
47. Khan, A.M.; Hussain, G.; Alkahtani, M.; Alzabidi, A.; Abidi, M.H.; He, N. Holistic sustainability assessment of hybrid Al–GnP-enriched nanofluids and textured tool in machining of Ti–6Al–4V alloy. *Int. J. Adv. Manuf. Technol.* **2020**, 1–13. [CrossRef]
48. Hong, S.Y.; Broomer, M. Economical and ecological cryogenic machining of AISI 304 austenitic stainless steel. *Clean Prod. Process.* **2000**, *2*, 157–166. [CrossRef]

49. He, L.; Chen, Y.; Li, J. A three-level framework for balancing the tradeoffs among the energy, water, and air-emission implications within the life-cycle shale gas supply chains. *Resour. Conserv. Recycl.* **2018**, *133*, 206–228. [CrossRef]
50. Jamil, M.; He, N.; Li, L.; Khan, A.M. Clean manufacturing of Ti-6Al-4V under CO_2-snow and hybrid nanofluids. *Procedia Manuf.* **2020**, *48*, 131–140. [CrossRef]
51. Khan, A.M.; Anwar, S.; Gupta, M.K.; Alfaify, A.; Hasnain, S.; Jamil, M.; Mia, M.; Pimenov, D.Y. Energy-Based Novel Quantifiable Sustainability Value Assessment Method for Machining Processes. *Energies* **2020**, *13*, 6144. [CrossRef]